Ultra-thin Strain Hardening Cementitious Composite (SHCC) layer in reinforced concrete cover zone for crack width control

He, Shan; Mustafa, Shozab; Chang, Ze; Liang, Minfei; Schlangen, Erik; Luković, Mladena

DOI
10.1016/j.engstruct.2023.116584

Publication date
2023

Document Version
Final published version

Published in
Engineering Structures

Engineering Structures 292 (2023) 116584

Contents lists available at ScienceDirect

Engineering Structures

journal homepage: www.elsevier.com/locate/engstruct

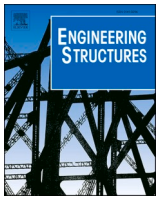

Ultra-thin Strain Hardening Cementitious Composite (SHCC) layer in reinforced concrete cover zone for crack width control

Shan He [a,*], Shozab Mustafa [b], Ze Chang [a], Minfei Liang [a], Erik Schlangen [a], Mladena Luković [b]

[a] Microlab, Faculty of Civil Engineering and Geosciences, Delft University of Technology, 2628 CN Delft, the Netherlands
[b] Concrete Structures, Faculty of Civil Engineering and Geosciences, Delft University of Technology, 2628 CN Delft, the Netherlands

ARTICLE INFO

Keywords:
SHCC
Crack width control
DIC
Lattice model

ABSTRACT

In the current study, experiments and numerical simulations were carried out to investigate the cracking behavior of reinforced concrete beams consisting of a very thin layer (*i.e.*, 1 cm in thickness) of SHCC in the concrete cover, tension zone. A novel type of SHCC/concrete interface that features a weakened chemical adhesion but an enhanced mechanical interlock bonding was developed to facilitate the activation of SHCC. The study involved testing hybrid SHCC/concrete beams that have various types of interfaces. The results were compared to the control reinforced concrete beams that do not have SHCC in the cover. Four-point bending tests were performed with the beams and Digital Image Correlation (DIC) was utilized to track the development of crack pattern and crack width. Results show that hybrid beams possessed similar load bearing capacity but exhibited a significantly improved cracking behavior as compared to the control beam. With a 1-cm-thick layer of SHCC, the maximum crack width of the best performing hybrid beam exceeded 0.3 mm at 53.3 kN load, whereas in the control beam the largest crack exceeded 0.3 mm at 32.5 kN load. The hybrid beam with the proposed new interface formed 10 times more cracks in SHCC than the hybrid beam with a simple smooth interface and had an average crack width less than 0.1 mm throughout the loading. The lattice model has successfully showcased its ability to predict and offer valuable insights into the fracture behavior of hybrid systems. The simulation results indicate that the presence of a weak interface bond, coupled with mechanical interlocking, can effectively facilitate the activation of SHCC, resulting in the formation of more cracks and a delayed progression towards the maximum crack width. As the volume ratio of SHCC used in the hybrid beams is only 6%, the current study highlights the strategic use of minimum amount of SHCC in the critical region to efficiently enhance the performance of hybrid structures.

1. Introduction

Concrete structures are designed to meet both ultimate limit state (ULS) and serviceability limit state (SLS) criteria. While the ULS addresses structural safety and stability, the SLS are essential for appropriate function and durability of concrete structures. Within the SLS design, the attention is paid particularly to the analysis and control of cracks. Cracking in concrete is an accepted phenomenon and does not have to cause problems if it remains within limits. These limits are laid down in codes describing what are acceptable crack widths for concrete structures in specific environments. Depending on the concrete mix composition, the reinforcement and the cover can thus be designed in such a way that the durability of the structure is secured within its designed service life. However, for infrastructure projects requiring extended service lives or operating in aggressive environments, substantial reinforcement is necessary to ensure an acceptable probability of having cracks remaining within the desired limits. Unfortunately, this often results in significant economic and environmental burdens.

Instead of designing reinforcement in excess of what the structural capacity demands, another strategy to control crack is by applying Fiber Reinforced Concrete (FRC). In recent years, the application of FRC in concrete structure/infrastructure has become increasingly popular [1–3]. Many research have demonstrated that FRC can significantly improve the behavior of structural elements at SLS with respect to crack width control [4,5]. Among all FRCs, the Strain Hardening Cementitious Composite (SHCC) or Engineered Cementitious Composite (ECC), initially developed in the 1990s based on the micro-mechanics theory [6], possesses the most desirable crack control ability as it can exhibit

* Corresponding author at: Stevinweg 1, 2628 CN Delft, the Netherlands.
E-mail address: s.he-2@tudelft.nl (S. He).

https://doi.org/10.1016/j.engstruct.2023.116584

Available online 13 July 2023

multiple micro-cracking behavior (*i.e.*, average crack width of 60–80 μm) with strain hardening response even at a tensile strain of more than 3% [7]. The ability to strain-hardening and to self-controlling the crack width makes SHCC a promising candidate for improving the resilience and durability of structural members. However, due to the high material cost of SHCC, complete replacement of reinforced concrete (RC) with SHCC is not economically feasible for most construction projects. Applying SHCC material only locally is a potential solution.

To investigate the possibility of combining SHCC and conventional concrete, various studies have developed hybrid systems using SHCC and RC for different structural members. These include the use of SHCC on the lateral surface of a beam for shear strengthening [8], on the tension side for flexural strengthening [9–11], or as a permanent formwork by pre-casting SHCC for the strengthening of both shear and flexural resistance [12]. Similarly, SHCC was also used together with FRP to form hybrid RC beam with enhanced flexural performance [13–15]. Furthermore, the same idea of combining SHCC with other material has also been employed with cold-formed steel to produce composite beams [16,17] and composite columns [18] with improved structural performance. Beside structural performance, the crack width control ability of SHCC/RC hybrid members was another focus [19]. Recently, the cracking performance of SHCC/RC hybrid beams under flexural loading was investigated [20]. The study adopted a 7-cm-thick layer of SHCC in the tensile zone of a 20-cm-high beam with reinforcement embedded in the SHCC and confirmed that the use of SHCC can sufficiently reduce crack width, thereby rendering the reinforcement design independent of the SLS criterion. However, the amount of SHCC used in this hybrid system is still relatively large, comprising 35% of the whole beam by volume. Given that the material cost of SHCC is roughly 3 times of the cost of reinforced concrete [21], a 35% concrete replacement ratio by SHCC will incur a significant amount of additional cost. For the other related research, the replacement ratio of the SHCC is usually higher than 35% and can sometimes go to more than 50%, which is even less economically attractive. It is, therefore, desirable to investigate the effectiveness of a SHCC/RC hybrid system with much reduced amount of SHCC.

In a hybrid element, the interface between different materials plays a crucial role in determining its performance. Many studies have therefore been conducted to enhance the integrity of concrete-to-concrete bonds [22,23]. Engineering methods such as roughening the existing concrete surface through high-pressure water jetting, sandblasting, or acid etching have been proposed [24]. Additionally, techniques like creating grooves [25], applying bonding agents [26], or incorporating steel reinforcement across the interface [27] have all been proven effective in improving the interfacial adhesion between concrete and concrete. However, the design of SHCC/concrete hybrid structural elements presents a challenge in terms of interface properties. This challenge arises due to the conflicting demands between preserving structural integrity and activating SHCC. While a strong interface is typically preferred to prevent delamination between the two layers, the formation of multiple cracks in SHCC necessitates a certain degree of laterally unrestrained deformation, which often requires a weak interface [25,28]. Consequently, a new type of interface between SHCC and concrete is needed to strike a balance between these conflicting demands.

The need for developing reliable models for structural interfaces and advanced modeling of hybrid concrete structures are widely recognized. Finite element analysis (FEA) is a widely used numerical technique for studying the mechanical response and performance of structures adopting novel material such as SHCC. Researchers have used FEA to study various aspects of SHCC structures, including the prediction of load–displacement responses [29,30], crack propagation patterns [31,32], and the influence of different parameters (such as fiber content, fiber type, and interface properties) on the performance of SHCC members [33]. Compared to FEA, discrete lattice models show advantages in terms of concrete fracture analysis, especially in modeling the crack propagation [34,35]. The lattice modeling approach is widely used in material research for simulating fracture [36] and even transport processes [37] in cement-based systems. Recently there has been some attempts in using the lattice modeling approach to simulate the structural behavior of reinforced concrete, which demonstrate the potential of using lattice model to explore and understand the fundamental mechanisms in structural members.

To solve the above-mentioned issues, a combined experimental and numerical study was carried out to investigate the cracking behavior of reinforced concrete beams consisting of a very thin layer (*i.e.*, 1 cm in thickness) of SHCC in the concrete cover zone. As part of a broader effort to improve the applicability and cost-effectiveness of concrete structures with self-healing ability [38], this study focuses on developing hybrid concrete beams featuring small cracks for an improved self-healing potential. In specific, to balance the conflicting requirements of maintaining structural integrity and maximizing SHCC activation, a novel interface design was developed. This design incorporates protruding teeth (shear-keys) on the SHCC surface and a Vaseline surface treatment (Fig. 1). The concept behind this approach is that the shear-keys offer mechanical interlocking to ensure overall structural integrity of the hybrid beams. Meanwhile, the Vaseline treatment allows the SHCC material between two lines of shear-keys to deform freely in relation to the concrete layer above it. In this way, a new interface condition which allows a controlled extent of partial delamination between the two layers can be achieved. For comparison purposes, interfaces with only the shear-key pattern but not the Vaseline treatment, as well as a smooth interface without any modification, were also made and applied to produce hybrid beams. The three hybrid SHCC/concrete beams with different interfaces were then tested and compared with a control reinforced concrete beam without SHCC. The beams were tested in four-point bending configuration, while Digital Image Correlation (DIC) was used to monitor the development of crack pattern and crack width. Furthermore, a fracture model (*i.e.*, a discrete type of lattice model [34]) was also used to acquire insight into the influence of the interface strength on the crack width and crack pattern of hybrid beams and to provide insights in how to further optimize the interface and thereby the behavior of the hybrid system.

2. Materials and tests

2.1. Experimental design

The experimental program consists of testing four 1.9-meter-long beams, including one conventional reinforced concrete beam as a reference specimen and three hybrid beams consisting of a 1-cm-thick SHCC layer in the tensile zone. The geometry and reinforcement details of the beams are given in Fig. 2. One hybrid beam has a smooth

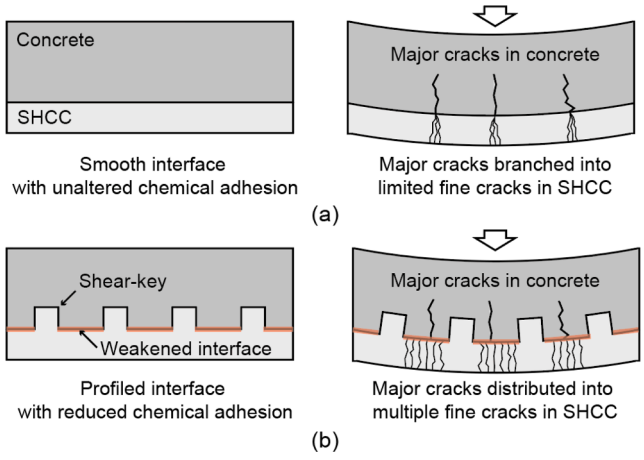

Fig. 1. Schematic illustration of (a) the smooth interface and (b) the proposed new interface with strong mechanical bond but weak chemical adhesion.

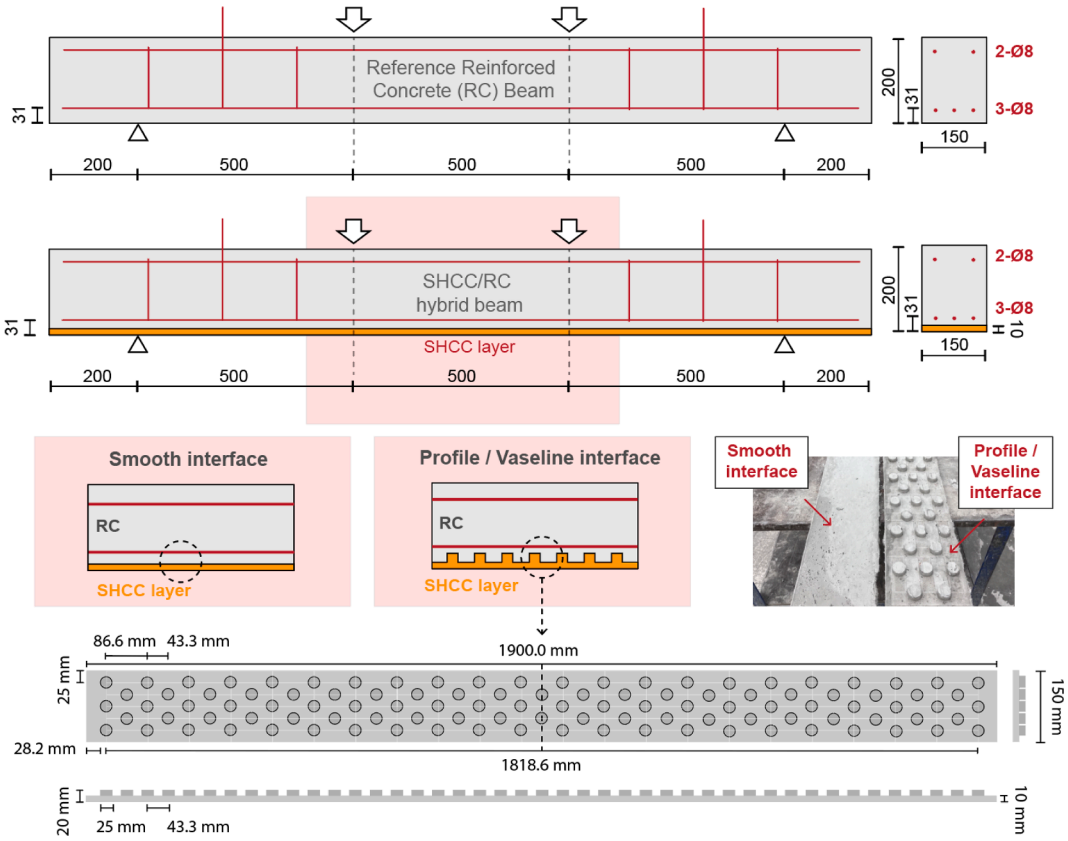

Fig. 2. Geometries and reinforcement details of the reference beam and the hybrid beams with different interface types. All dimensions are in mm.

interface between SHCC and reinforced concrete, while the other two hybrid beams have a profiled interface, which is made of a pattern of protruding teeth (shear-key) from the SHCC layer. The interface pattern consists of equally sized and evenly spaced cylindrical keys, which have a diameter of 2.5 cm and a height of 1 cm. The clear distance between 2 adjacent keys is 2.5 cm, which is selected such that the largest aggregate in the concrete can fill into the gap. The shear-keys are designed to provide adequate mechanical interlocking between the SHCC and the concrete layers so to ensure the structural integrity of the hybrid system. The image at the bottom of Fig. 2 shows the design of the shear-key pattern. Furthermore, within the two hybrid beams having profiled interface, one beam has a purposely weakened interfacial bond, which was realized by applying a thin layer of liquid Vaseline on the profiled side of the SHCC laminate. This treatment is to reduce the chemical adhesion between SHCC and concrete and to promote local debonding. The aim for combining the Vaseline treatment and the shear-key profile is to fully utilize the tensile strain capacity of the SHCC by allowing a controlled degree of differential deformation between the SHCC and the concrete, as schematically illustrated by Fig. 1. In the following text, the reference beam is referred as Ref and the hybrid beams with smooth interface, profiled interface and Vaseline treated profiled interface are referred as Smooth, Profile and Vaseline, respectively.

The geometry of the beams was adopted from previous studies [10,20]. The beams are 1900 mm long, 150 mm wide and 200 mm high. For the hybrid beams, the bottom 10 mm of concrete is replaced by SHCC. The reason why the hybrid beams in the current study only have the SHCC layer in the bottom cover is for easy examination of the different crack patterns in SHCC and in concrete. Cracks on the front and back sides of the beams are not considered to govern the durability, because the SHCC layer will eventually be applied in the 4-side cover zone of the entire beam for an all-around protection. All the beams have the same reinforcement configuration with 3 Φ8 ribbed rebars at the bottom and 2 Φ8 ribbed rebars at the top (as shown in Fig. 2). The clear cover depths for all the beams are 31 mm. To allow the development of cracks in the constant moment region, the percentage of longitudinal reinforcement was kept low (0.61%). The stirrups of Φ8@150 are provided in the shear span to ensure that the beams fail in flexure. The central stirrup on both sides is extended upward for easy handling of the beams.

2.2. Materials and sample preparation

Table 1 shows the mixture compositions of SHCC used in the current study. The mix design of the SHCC was developed in the group previously [39,40] and features a high tensile strain capacity of more than 4% under direct tensile test after 28 days of moisture curing. The SHCC matrix was produced with a filler-to-binder ratio of 0.5 and a water-to-binder ratio of 0.4, using blast furnace slag (BFS) cement CEM III/B 42.5 N from ENCI (the Netherlands) as the binder and finely ground limestone powder Calcitec® from Carmeuse (Belgium) as the filler. A polycarboxylate-based superplasticizer called MasterGlenium 51, manufactured by BASF (Germany) with 35.0% solid content by mass, was added to achieve the desired workability. The fiber used in this SHCC mixture is Polyvinyl Alcohol (PVA) fiber at an amount of 2% by volume.

Table 1
Mixture compositions of SHCC and concrete [unit in kg/m3].

Material	SHCC	Concrete
CEM I 52.5 R	–	260
CEM III/B 42.5 N	1060	–
Limestone powder	530	–
Sand (0.125–4 mm)	–	847
Gravel (4–16 mm)	–	1123
PVA fiber	26	–
Water	424	156
Superplasticizer	2	0.26

The fiber was sourced from Kuraray (Japan) with 1.2% oiling coating by weight, and its mechanical and physical properties are presented in Table 2. The mixture composition of concrete is also provided in Table. 1.

All the hybrid beams in the current study were cast in 2 steps. In the first step, smooth SHCC laminates were cast vertically by using a plywood mold (Fig. 3a) having pockets/slots with an opening of 10 mm. As compared to casting the SHCC laminates in the lie-flat manner, casting a thin laminate vertically allows a more precise control on the thickness of the laminate, which is vital to the current study. The SHCC laminates with shear-keys were prepared by a similar mold but with an opening of 20 mm (Fig. 3b). The 20-mm-thick slot contains a 10-mm-thick silicon rubber glued to one side wall having a reverse shape of the desired shear-key pattern (Fig. 3c). By casting the SHCC into the remaining gap, the fresh material will fill into the holes of the rubber sheet and then form the resulting protruding keys as shown by Fig. 3d. All the laminates were cured for 14 days in a climate room (20 °C and ≥ 98% RH) before casting of concrete. In the second step, SHCC laminates were taken out from the climate room and placed into plywood mold. On top of the SHCC laminates, reinforcement cages were placed with appropriate spacers. After the preparation, the concrete was cast and compacted using a vibration needle. The hybrid beams were then cured for 28 days in sealed conditions before testing. The reference reinforced concrete beam was cast along with this second phase.

To prepare the SHCC materials, dry powders were first mixed by a Hobart® mixer for 5 min. Water pre-mixed with 80% of SP was slowly added into the mixture and mixed until the fresh paste was homogenous and consistent, followed by the addition of fibers within a duration of 5 min. Meanwhile, the remaining 20% SP was added into the mixture to compensate for the rheological loss due to the addition of fibers. Afterward, the fresh SHCC was cast into the special molds for the laminates, as well as into polystyrene prism molds and dog-bone molds for the determination of compressive and tensile properties of the SHCC material. All the casting work was performed on a vibration table to remove entrapped air and to improve the filling of fresh SHCC into the holes of the rubber sheets. The materials were then covered with plastic sheets and cured at room temperature for one day, after which the hardened specimens were removed from the molds and cured in a climate room (20 ℃ and ≥ 98% RH) for another 14 days. After the specimens were removed from the climate room, the SHCC laminates were placed into the beam molds for the preparation of hybrid beams, and the dog-bone and prism specimens were sealed with plastic bag. This is to ensure that the curing histories of the dog-bones and prisms are comparable to that of the SHCC laminates in the hybrid beams. Concrete cubes of 150 mm × 150 mm × 150 mm were prepared following NEN-EN 12930–3 [41] to determine the compressive strength of concrete.

2.3. Testing

All the beams were tested in a four-point bending test setup (Fig. 4a) under displacement control at a rate of 0.01 mm/s. The deformation of the beams was monitored within the constant bending moment region by using Digital Image Correlation (DIC) for both sides, while the relative vertical mid-point deflection of the beams with reference to the supports was measured by a Linear Variable Differential Transformer (LVDT). DIC is a measurement technique that processes pictures taken from cameras to track and record the surface motion of a deforming solid. The regions of the beam for DIC measurement were first painted in white and sprayed with a black speckle pattern by using an air gun. Images for DIC were captured throughout the loading at 10-second intervals at a resolution of 0.08 mm/pixel. Post-processing of DIC results was carried out with a free version of GOM Correlate software.

The compressive strength of the SHCC was measured in accordance with NEN EN 196–1 [42] by using 40 mm × 40 mm × 40 mm cube specimens cut from prism specimens. Uniaxial tension tests were performed by using a servo-hydraulic testing machine (Instron® 8872) under displacement control at a rate of 0.005 mm/s. Dog-bone shaped specimens recommended by the Japan Society of Civil Engineers (JSCE) [43] with a cross-section of 13 mm × 30 mm at the test zone were adopted. During tests, the specimens were placed inside of a pair of tensile grips and then slightly pre-stressed before testing. The deformations were measured with a gauge length of 80 mm with two LVDTs fixed on both sides of the specimens as shown by Fig. 4b. Tests were stopped by releasing the applied tensile load after the tensile load dropped to less than 50% of the maximum load. The maximum tensile stress experienced by the specimen during this experiment is called the ultimate tensile strength (σ_{ult}), and the strain value when the load drops to 90% of the ultimate value is taken as the tensile strain capacity (ε_{ult}). Four samples were tested for the determination of the tensile properties of SHCC. The average and the standard deviation of the results are reported.

Table 2
Physical and mechanical properties of PVA fibers.

Length (mm)	Diameter (μm)	Density (kg/m3)	Nominal tensile strength (MPa)	Young's modulus (GPa)	Surface oil-content (wt. %)
8	39	1300	1640	41.1	1.2

3. Experimental results

3.1. Material properties

Fig. 5 shows the typical tensile stress–strain curves of SHCC dog-bones cured comparably to the SHCC laminates in the hybrid beams. The tensile testing process of SHCC consists of three phases. In the first phase, the material undergoes a linear elastic phase, characterized by a straight line with a slope equal to its Young's modulus. In the second phase, cracks begin to successively form while load continues to increase. This phase is characterized by the sequential formation of multiple parallel cracks, which results in temporary load drops and contributes to inelastic deformation. The final phase is marked by the occurrence of the final fracture, which signals the exhaustion of the fiber-bridging capacity of the composite and defines its ultimate strength. As can be seen, the mixture exhibited pronounced tensile strain hardening behavior with the formation of multiple fine cracks as shown by the inset of Fig. 5. Table 3 summarizes the mechanical properties of SHCC and concrete. The average tensile strain capacity of SHCC is 3.2% and the average tensile strength is 4.1 MPa. The average compressive strengths of SHCC and concrete are 67.5 MPa and 47.5 MPa respectively. The adoption of a relatively stronger SHCC as compared to concrete is to ensure that the thin laminates can withstand the loads caused during demolding, handling and beam casting. A stronger cover zone with dense micro-structure is also expected to be favorable to the durability of a structural element.

3.2. Structural behavior

Fig. 6 shows the comparison of load deflection response and maximum crack width development between the beams. As can be seen from the solid lines, load–deflection curves of the hybrid beams were in general similar to the curve of reference reinforced concrete beam. Only that the first-cracking loads of all the hybrid beams were slightly higher than that of the reference beam, which is expected given that the SHCC can provide additional bridging force even after the concrete is cracked. After cracking, the stiffness of the beams was reduced and no significant difference between the stiffness of the hybrid beams and the reference beam can be noticed. The next turning point is when the load ceased to increase linearly with increasing deflection, which marks the starting point of reinforcement yielding. In this stage, a slightly more

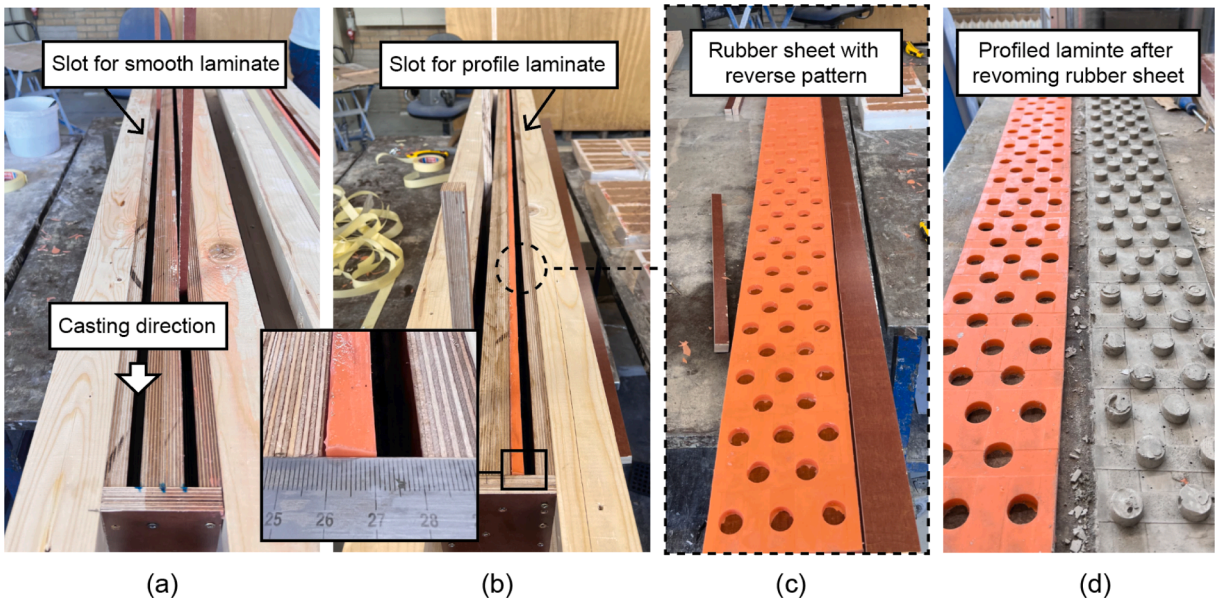

Fig. 3. Wooden mold for the preparation of (a) SHCC laminate with smooth surface and (b)-(c) SHCC laminate with a profiled surface, as well as (d) a SHCC laminate with profiled surface rightly after demolding.

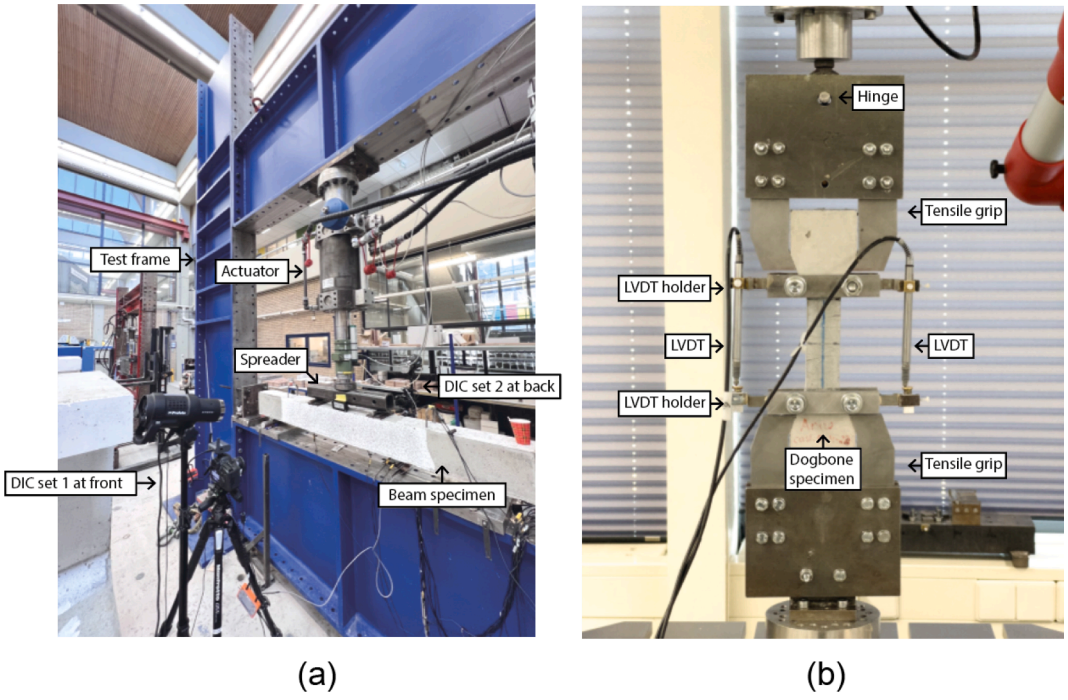

Fig. 4. Experimental set-up for (a) four-point-bending test of beam specimens with DIC measurement on both sides and (b) uniaxial tensile test of SHCC dog-bone specimens.

pronounced tension hardening behavior can be noticed for the hybrid beams compared to reference beam due to the contribution of SHCC in tension. The last stage is when the load started to decrease as marked by the square markers on the curves, which indicates the onset of the failure stage of the beams. As can be seen, all the tested beams have similar load carrying capacity. While the maximum load for the Ref beam is 58.9 kN, the load bearing capacity for the Smooth, Profile and Vaseline hybrid beams are 58.2 kN, 59.7 kN and 57.7 kN, respectively. The difference is only 3 percent over the highest load value. This is as expected because all the beams have the same reinforcement and the contribution from the 1-cm-thick SHCC layer to the resistance moment is small.

Still, the curves after the reinforcement yielding are noticeably different depending on the interface type. For the Ref and Smooth beams, the loads increased monotonously with increasing deflection, followed by a quick drop after reaching the ultimate load. On the contrary, the loads of the Profile and the Vaseline beams first increased and then decreased at an almost identical speed for a similar amount of deflection, displaying a roughly symmetric and concave shape along the vertical line passing the maximum point. This difference means that the Profile and Vaseline beams reached their maximum loads at much smaller deflections than the Ref and Smooth beams. As compared to the Smooth beam whose mid-point deflection is 26.4 mm when the load is at

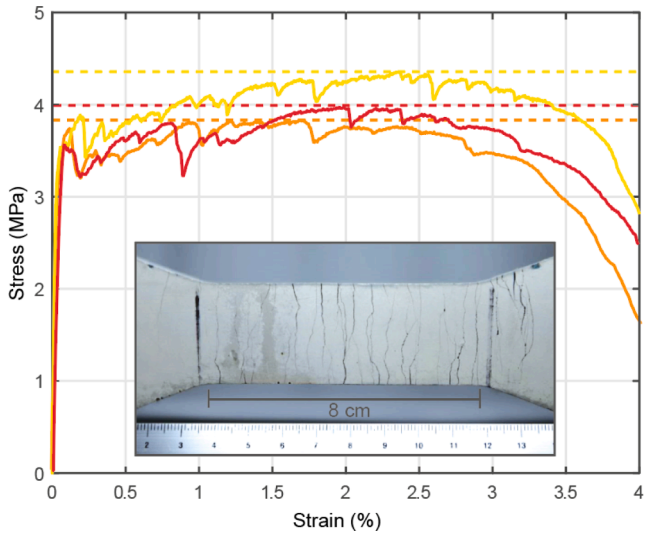

Fig. 5. Stress–strain curves of SHCC under direction tension with an inset image showing a typical crack pattern of a dog-bone specimen after test.

Table 3
Results of uniaxial compression and tension tests.

Mixture	Compressive strength (MPa)	First cracking strength (MPa)	Ultimate tensile strength (MPa)	Ultimate tensile strain
SHCC	67.5 ± 0.7	3.7 ± 0.3	4.1 ± 0.4	3.2%±0.7%
Concrete	47.9 ± 2.0	–	–	–

its maximum, the equivalent deflection for the Vaseline beam is only 14.3 mm. This is probably because that, in the beams with a profiled interface, the cracks in concrete developed at lower loads for that the shear-key might have provided a splitting force to open up a crack, resulting in an early crack localization and an accelerated elongation of the reinforcement. Also because of the presence of the shear-key, the crack patterns in the SHCC are much more complex in the hybrid beams with profiled interface as shown by Fig. 7. It is thus possible that the SHCC was activated earlier than the Smooth and Ref beams as a result of the stress concentration and the additional tensile force developed due to the shear-keys.

More importantly for the aim of this study, it can be seen from the dashed lines in Fig. 6a that all hybrid beams show improved crack width control ability. The dashed lines in Fig. 6a show the development of the maximum crack widths along the bottom edge of the beams with increasing deflection as calculated from the DIC results from both the front and back sides of the same beam. The maximum values were taken from the side with larger crack widths. As can be seen, the reference beam showed maximum crack widths exceeding 0.3 mm at a load of 32.5 kN. In contrast, the hybrid beams with smooth, profiled, and Vaseline-applied profiled interfaces were able to contain crack widths below 0.3 mm until loads of 40.6 kN, 51.0 kN and 53.3 kN, respectively. This paper adopted a surface crack width limit of 0.3 mm, which is the prescribed threshold in Eurocode 2 [44] for reinforced concrete under quasi-permanent load across all exposure classes, except for X0 and XC1. For the best performing hybrid beam (*i.e.*, the Profile beam), its load at 0.3 mm crack width reaches 89.3% of its ultimate capacity. Fig. 6b summarizes the loads and deflections for the tested beams when the maximum crack width reached 0.3 mm. Though the hybrid beams all exhibited a deferred opening of cracks in SHCC, it is obvious that the hybrid beams with a profiled interface (*i.e.*, the Profile and Vaseline beams) have a superior crack width control ability. Not only the loads at 0.3 mm crack width of the Profile and Vaseline beams were higher than the Smooth beam, a 0.3-mm-wide crack also happened at a much larger deflections for the Profile and Vaseline beams (*i.e.*, at 6.2 mm and 6.3 mm respectively) as compared to the Smooth beam which reached the 0.3 crack width at only 3.6 mm. This deflection value is only slightly higher than that of the Ref beam, showing that the crack width control ability of the SHCC material was only marginally activated in the Smooth beam.

To further investigate the different behaviors of the hybrid beams in terms of the crack development, the evolution of crack pattern in the constant bending moment region at 30 kN, 50kN and ultimate load for all the tested beams are shown in Figs. 8-10. The crack patterns are obtained by DIC principal strains analysis with a unit in percentage. The moments at which the crack patterns were recorded are shown by the circle markers at the load–deflection curves next to the respective crack pattern image. As shown by the crack patterns, all beams exhibited first flexural cracking, followed by crack opening and then a final failure of concrete in the compression zone. By comparing Fig. 8a and 8b, it is found that the SHCC layer has very little influence on the cracking behavior of the beam when a smooth interface is adopted. Branching of cracks from concrete to SHCC was observed only to a very limited extent as shown in Fig. 11a and 11b, which are zoom-in images of the strain field at the SHCC/concrete interface. The locations from where the images were captured are marked in the crack pattern of Smooth beam

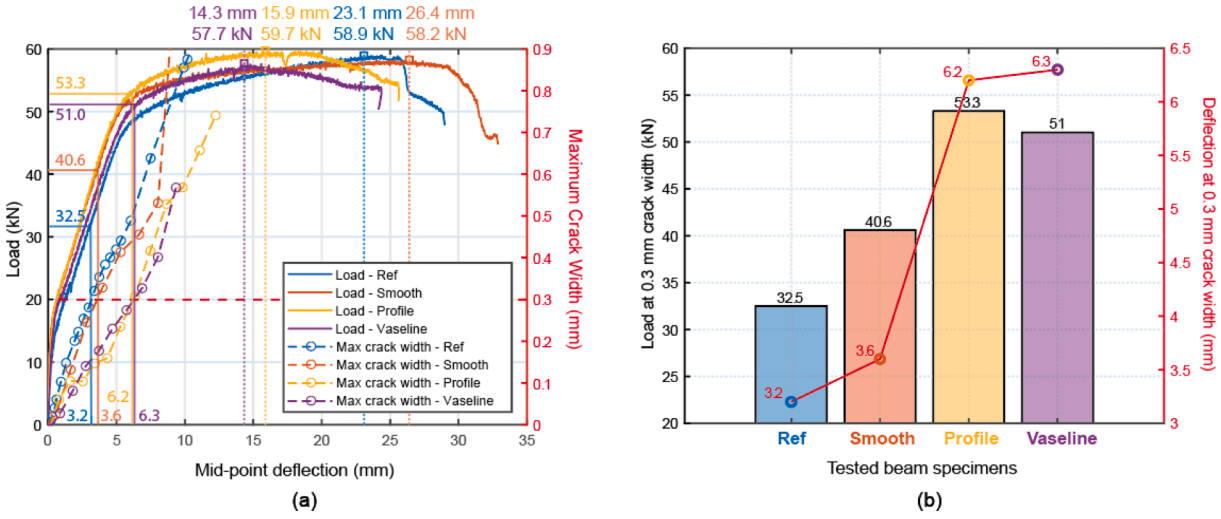

Fig. 6. (a) Load-deflection-crack width response of all tested beams and (b) summary of load and deflection values when the maximum crack width exceeds 0.3 mm for each beam.

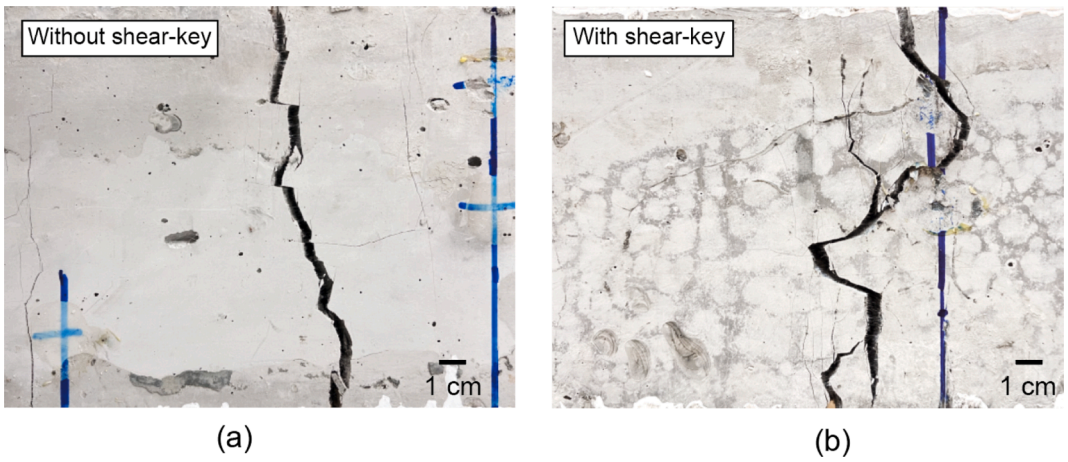

Fig. 7. Crack pattern of the bottom side of (a) Smooth beam and (b) Vaseline beam.

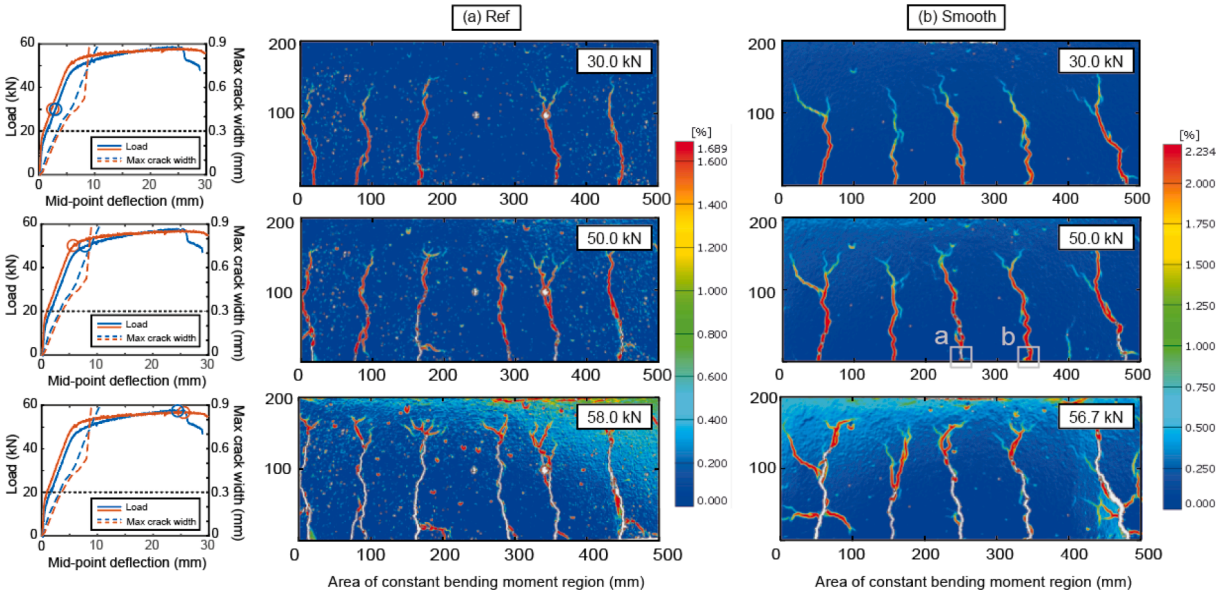

Fig. 8. Crack pattern development at 30 kN, 50kN and ultimate load for (a) Ref beam and (b) Smooth beam.

(Fig. 8b) at 50 kN. As can be seem from the zoom-in images, cracks from concrete can be spread into only 2–3 smaller cracks in SHCC and no delamination can be observed between the 2 layers, resulting in an extremely narrow cracked zone in the SHCC. This indicates that the adhesion between SHCC and concrete at smooth interface is so strong that the debonding is thoroughly resisted, causing only a small portion of SHCC to be activated and an early localization of cracks in SHCC. This restricted crack-distributing behavior also explains the limited crack width control ability of the SHCC layer in the hybrid beam with a smooth interface.

Fig. 9 and Fig. 10 show the crack pattern of the hybrid beams with profiled interface (*i.e.*, Profile and Vaseline beams). The vertical lines in white color in the crack pattern images show the positions of the cracks in the SHCC along the length of the constant bending moment of a beam. As can be seen, both beams exhibited considerably more cracks in the SHCC as compared to the Smooth beam. Unlike the crack pattern of the Smooth beam, the thin SHCC layer with a distinct cracking behavior from that of concrete can be easily noticed at the bottom of the Profile and Vaseline beams. The zoom-in images at the Concrete/SHCC interface (Fig. 11c, 11d and 11e) also show that the cracks from concrete were largely arrested in both the Profile and Vaseline beams and that the branching of cracks were much more obvious than that of the Smooth beam. The reason for the better crack performance of the SHCC with a profiled interface is probably that the presence of shear-keys can lead to a non-uniform load transfer between the concrete and the SHCC layer. In such a case, stresses may have concentrated around the shear-keys even at a low load level and thus leaded to a relatively early local delamination near shear-keys as shown by the crack patterns at 30 kN, which then facilitated the activation of SHCC and the formation of micro-cracks. It might also be that, due to interlocking profiles, more cracks in concrete can be triggered and thus results in smaller crack width in concrete, which will certainly ease the burden of SHCC to distribute the concrete cracks locally. Furthermore, because of the additional shear stress taken by the shear-key, the tensile stress in the SHCC layer is expected to be higher than that of a smooth interface, which may have further encouraged cracking in the SHCC.

In addition, by comparing the crack patterns between the Profile beam and the Vaseline beam, it can also be found that a higher portion of the SHCC was activated in the Vaseline beam than the Profile beam. By comparing the zoom-in images of the Profile beam (Fig. 11c and 11d) and the Vaseline beams (Fig. 11e), it can be found that delamination between SHCC and concrete is more pronounced in the Vaseline beam than in the Profile beam, which might have led to the activation of a wider portion of SHCC and the formation of more cracks. As can be seen

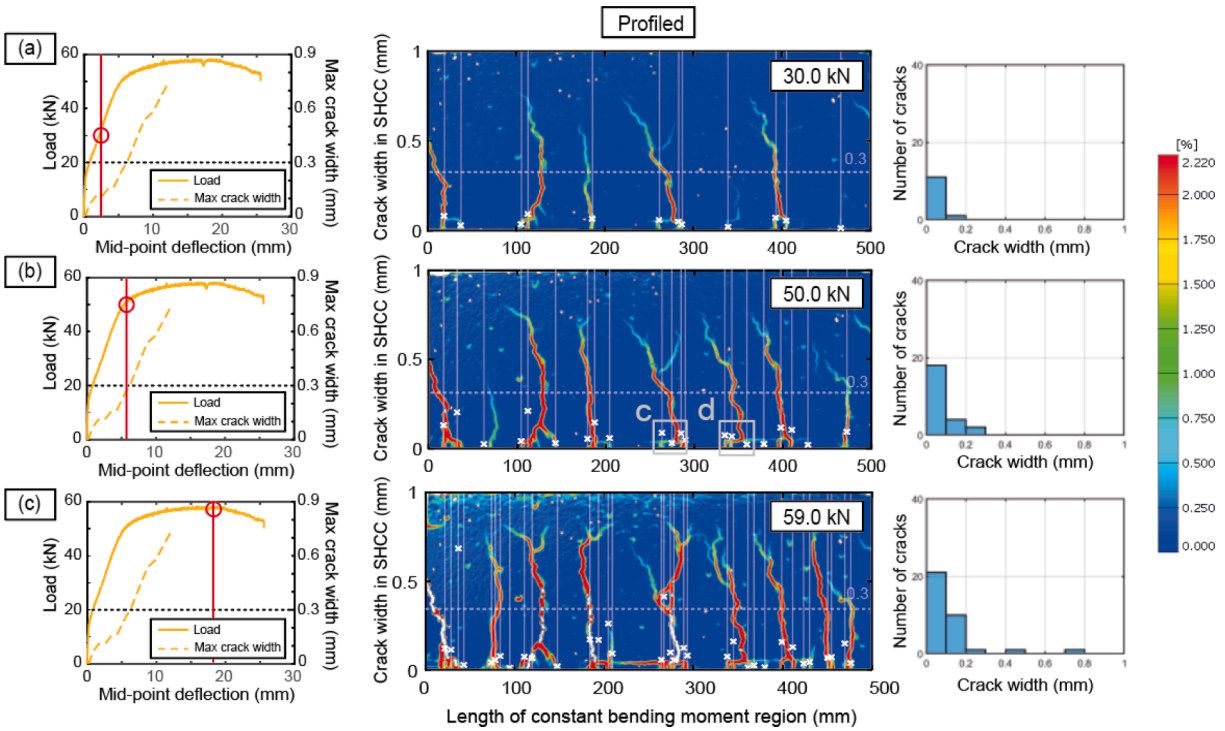

Fig. 9. Crack pattern development of the Profile beam at 30 kN, 50kN and ultimate load as well as the crack width distribution at each load levels. The vertical lines in white color show the positions of cracks in the SHCC; and the y-value of each '×' marker is the crack width of each individual crack.

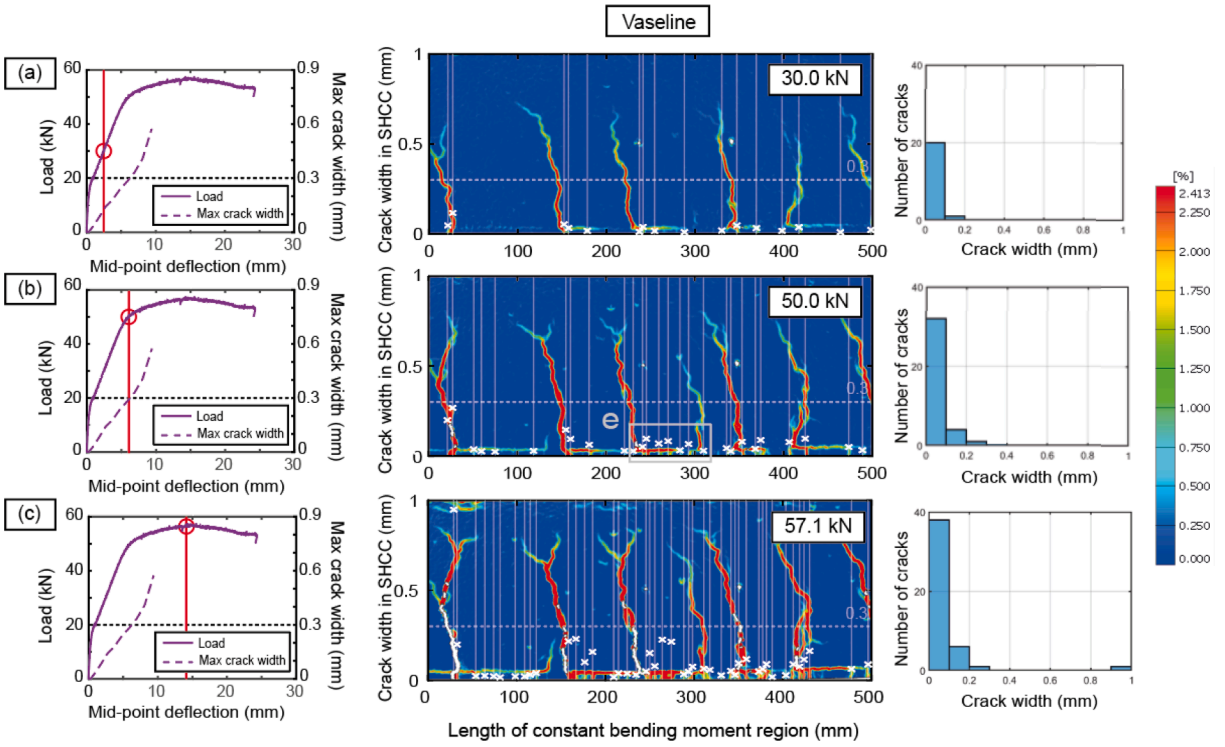

Fig. 10. Crack pattern development of the Vaseline beam at 30 kN, 50kN and ultimate load as well as the crack width distribution at each load levels. The vertical lines in white color show the positions of cracks in the SHCC; and the y-value of each × marker is the crack width of each individual crack.

from the histograms right to the crack pattern in Figs. 9 and 10, the number of cracks in the SHCC layer of the Vaseline beam is almost two times that of the Profile beam for all the three load levels. This demonstrates that a purposely weakened interface can indeed facilitate the activation of SHCC in a hybrid structure by allowing differential deformation between the SHCC and concrete layers.

The width of the cracks formed in the SHCC layer of the hybrid beams were also calculated and overlapped over the crack pattern images as the cross makers in Figs. 9 and 10. The y-values of the makers represent the individual crack width while the x-values correspond to

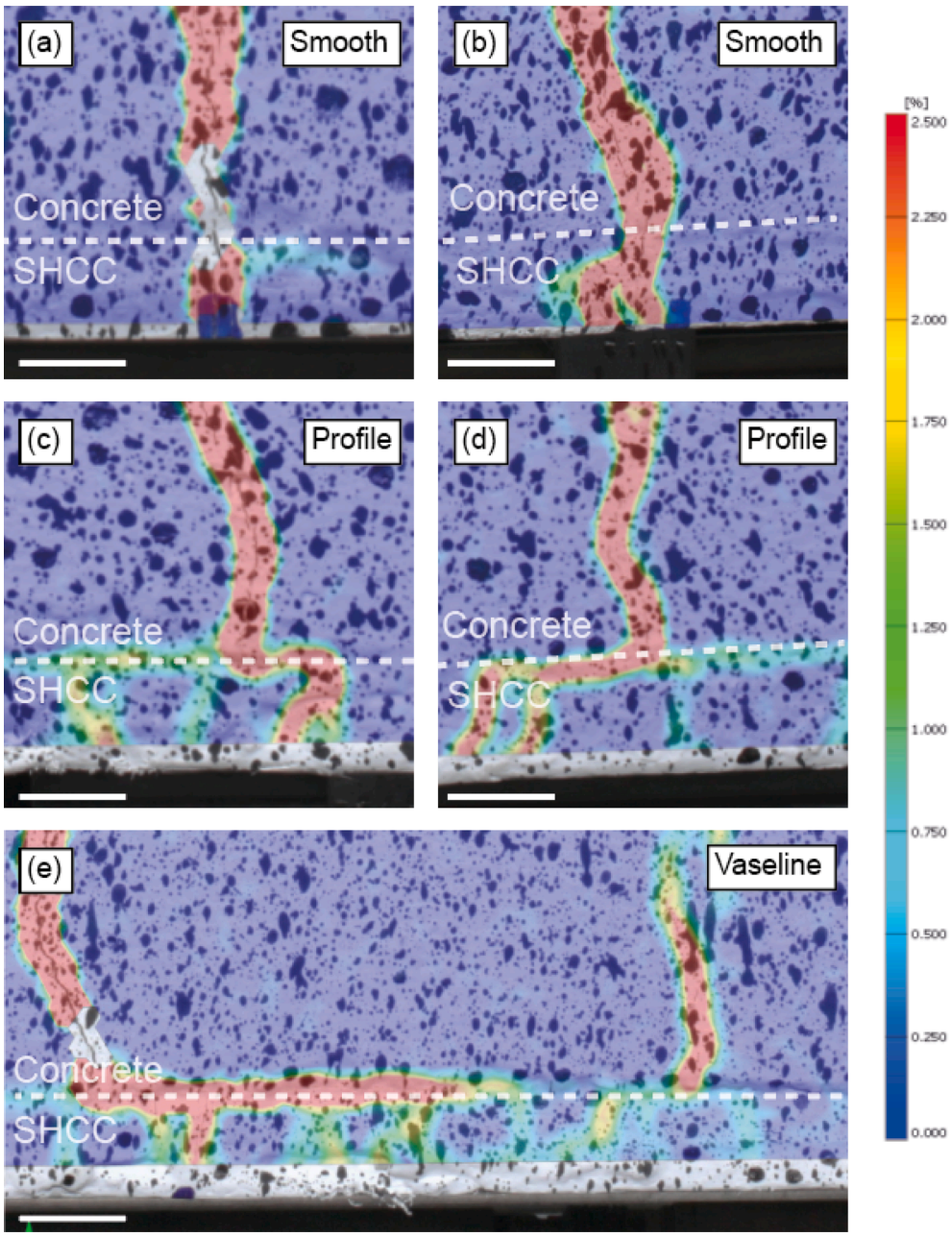

Fig. 11. Zoom-in images of the crack pattern at interface between concrete and SHCC for all the hybrid beams at 50 kN load. Scale bar = 1 cm.

the locations of each crack along the beams. From the figures, it can be clearly seen that the majority of cracks formed in SHCC are micro-cracks smaller than 0.3 mm even at the ultimate loads. Also, it can be found that even though the localized cracks were widened significantly at high loads, most of the cracks formed in SHCC stayed small (*i.e.*, to well below 0.3 mm) for all load levels. Fig. 12a and 12b quantitatively show the distribution of crack width in the Profile and the Vaseline beams with increasing deflection. As can be seen, though the maximum crack width increased quickly with increasing deflection, the average crack width stayed stable around 0.1 mm. Except for only a few cracks that went larger than 0.3 mm, most of the cracks remained below 0.2 mm wide.

Fig. 13a shows a comparison of average crack width between all the tested beams. Unlike the Profile and Vaseline beams, the average crack widths for the Ref and Smooth beams increased almost linearly with increasing deflection, which again proves that a smooth interface in a SHCC/RC hybrid system is not desirable as the crack control ability of SHCC cannot be sufficiently triggered. Besides, it can be seen that the Vaseline beam has the lowest average crack width among the 4 tested beams, which should be a direct result of having more cracks. Since the safety and reliability of a structure are typically evaluated using a probabilistic approach, it can be concluded that the Vaseline beam is the best performing beam as it has the lowest probability of surpassing the crack with limit of SLS. This is due to its superior performance in restricting both the 'maximum' and 'average' crack widths, ultimately resulting in a reduced likelihood of exceeding the limit state.

Fig. 13b shows the change of crack number with increasing deflection for all the beams. As expected, the Vaseline beam has the highest number of cracks for almost the entire test period. The max crack number of the Vaseline beam is about 160% of that of the Profile beam and 10 times more than the Smooth and Ref beams. Furthermore, it can also be seen that the crack number of Vaseline beam kept increasing until a much larger deflection than the rest of the beams. While the Ref and the Smooth beams stopped forming more cracks at a deflection around 3 mm, the Vaseline beam reached its maximum crack number at

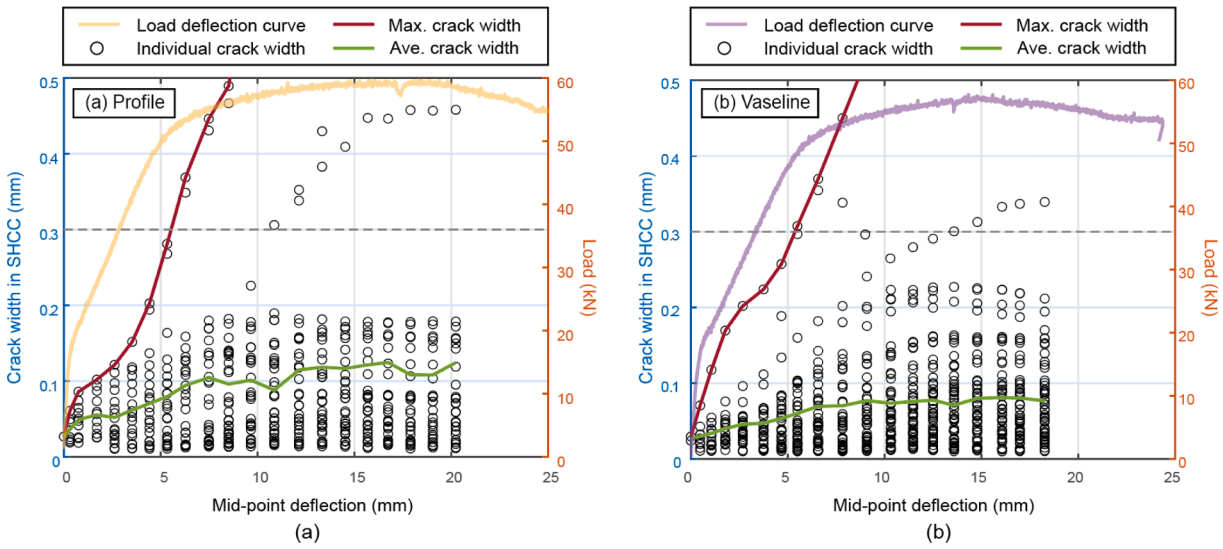

Fig. 12. Crack width distribution for (a) Profile beam and (b) Vaseline beam.

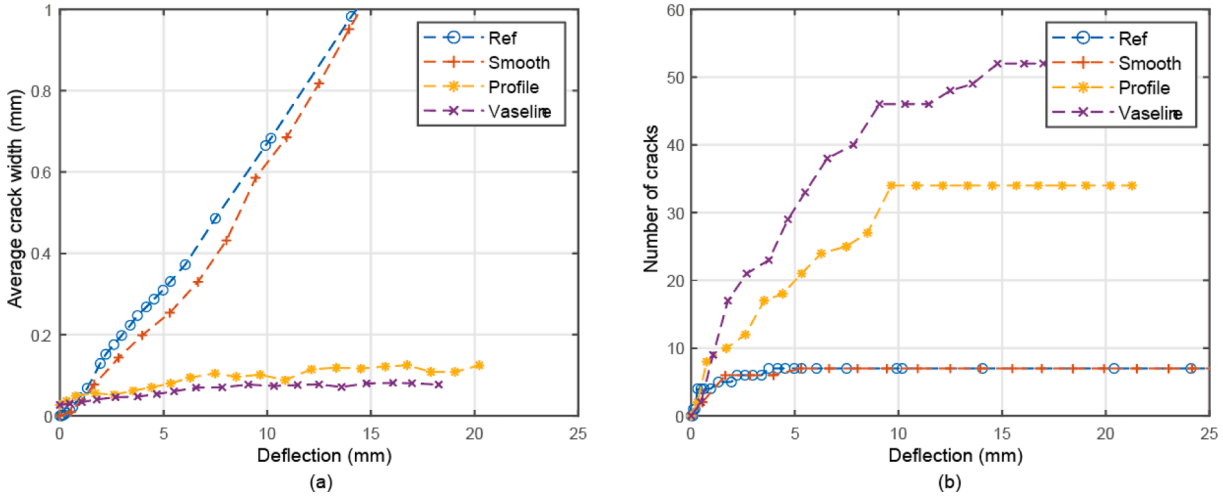

Fig. 13. Comparison of (a) average crack widths and (b) number of cracks between all tested beams.

a deflection of 15 mm, which is also much larger than the 10-mm-deflection at which the Profile beam stopped generating more crack. The superior performance of the Vaseline beam again demonstrates the advantage of having a chemically debonded but mechanically connected bond behavior to the crack width control performance of SHCC/RC hybrid structural elements.

One possible issue with the use of a purposely weakened interface for a hybrid structure is the risk of having complete delamination, which might severely damage the structural integrity. To investigate the extent to which the delamination was influenced by the Vaseline treatment, the deformation of the Profile and Vaseline beams in y-direction from the DIC analysis at different load levels is presented in Fig. 14. To highlight the delamination degree, only the lower parts of beam near the interface, instead of the full height of the beam, are presented. The relative y-direction displacement between the 2 layers at several critical sections (as marked by the dashed lines) are also given in the line plot below the respective DIC images. As can be seen from the DIC strain fields in Fig. 14a and 14b, the Vaseline treatment has indeed led to a wider range of delamination even at lower deformation. However, a full delamination did not occur as the two layers were still tightly bonded at some locations along the interface, where the shear-keys might stay. Fig. 14 also shows the opening of interface at several critical sections as marked by the dashed line, as referred by P1-5 and V1-5 in the Profile and the Vaseline beam, respectively. As can be seen, both beams exhibited a controlled degree of delamination, *i.e.*, the opening of the interface remained stable with increasing deflection. However, it can be seen that the maximum opening of interfacial crack of the Vaseline beam experienced an abrupt increase when deflection reached around 16 mm. This is because at this moment the beam has already passed its ultimate load and the crack in SHCC has started to localize fast. Still, it can be observed that, as long as the Vaseline beam did not reach its ultimate load (ULS scenario), the opening of interface crack was restricted below 0.3 mm, securing the structural integrity of the hybrid system.

Based on the above experimental results, it can be concluded that a 1-cm-thick SHCC layer can be very effective in controlling the crack width of a hybrid beam, as long as the interface is properly designed. The new interface type of having a shear-key pattern and a layer of Vaseline is also successfully demonstrated to enable a tailored bonding mechanism. However, it is still not clear to what extent has the Vaseline treatment reduced the interface bond and whether it is beneficial for the interface properties to be as weak as possible. Application of numerical testing, validated with experimental observations, might be beneficial as it can provide insights into the influence of a single parameter which is difficult to precisely control in an experimental study. It is thus decided to

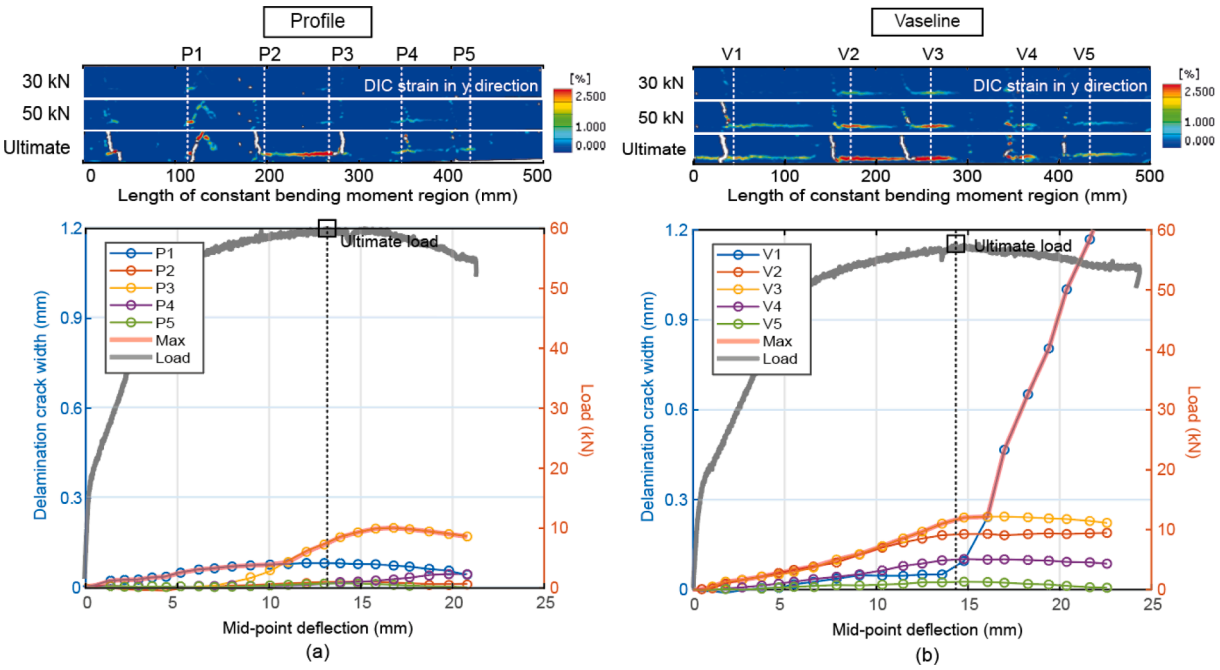

Fig. 14. DIC strain in vertical direction near the RC/SHCC interface at 30kN, 50kN and ultimate load as well as the vertical opening of delaminated positions for (a) Profile beam and (b) Vaseline beam.

conduct numerical study to answer the above-mentioned questions.

4. Numerical simulations

4.1. Introduction

The lattice modeling approach has been extensively utilized in material research to simulate various phenomena in cement-based systems, including fracture [34,35], moisture transport [45], chloride diffusion [37] and 3D printing process [46]. Recently, the lattice model was also extended to simulate the structural behavior of reinforced concrete structural elements [20,47]. Adopting a similar approach, the lattice model was also used in the current study to examine the cracking behavior of the SHCC/RC hybrid beams. The aim of this numerical study is to quantitatively investigate the influence of interface properties on the activation of SHCC and on the crack width development.

In a lattice model, the material is discretized as a network of truss or beam elements connected at the ends. In most cases, elements have linear elastic properties. In each loading step, the element having the highest stress-to-strength ratio is removed from the system. The system is then updated due to the damage of losing one element. The analysis procedure is repeated until a pre-determined failure criterion (*i.e.*, in term of either load or displacement) for the simulated specimen is achieved. In certain situations where plasticity has to be introduced (*e.g.*, elements of reinforcement, the interface between steel and concrete, and SHCC), multi-linear constitutive relationship is assigned to those elements as pairs of stiffness and strengths. Each pair represents a point on the stress–strain curve of the material and is referred as a segment. For those elements, the stiffness decreases gradually when the stress in an element reaches its strength. This occurs by moving from one segment to the next, in contrast to the complete removal from the mesh for (brittle) materials having single segment. In this way, stress–strain responses and realistic crack patterns of both brittle and ductile material can be obtained. For a detailed description on the procedure of constructing a lattice model for structural application, please consult [20].

To build lattice models of hybrid beam with a profiled interface, SHCC laminates with shear-keys were first modelled in lattice. Due to the limitation of the mesh size (*i.e.*, 10 mm), the cylindrical shear-keys were modelled as prisms following an equivalent pattern as shown in Fig. 15a. The resulting lattice model of a profiled SHCC laminate can be seen as Fig. 15b. The length of the simulated SHCC laminate is 1.5 m so that only the effective span of the beam is modelled. Fig. 15c shows the resulting model of a hybrid beam. The model consists of 5 types of elements, namely Concrete, SHCC, Reinforcement, SHCC/Concrete Interface and Concrete/Reinforcement Interface. A total of six simulations were carried out in this study, including one reference reinforced concrete beam (designated as R) and five hybrid beams. Within the five hybrid beams, one beam is with a smooth interface (designated as S), while the remaining four beams are with a profiled interface but with different SHCC/Concrete interface properties (designated as P75, P50, P25 and P10, with reducing strength of interface elements). A list of the simulated models can be found in Table 4.

4.2. Model inputs

The lattice elements are assigned mechanical properties (*i.e.*, stiffness and strengths) based on the materials they represent. In this study, all lattice elements are cylindrical and have a circular cross-section. The radius of these elements is determined iteratively to match the global elastic modulus obtained in the lattice simulation with the input of elastic modulus in a direct tension test. This iterative process ensures that the stiffness of the members is simulated accurately. The strengths in the lattice model are determined by inverse modeling, which means that they are adjusted such that the response of the simulated test matches the experimental results [36]. Table 5 shows a list of input properties for lattice simulation. The compressive strength of concrete is simulated to be 47.5 MPa based on experimental results. Although the tensile strength and elastic modulus of concrete are not directly tested, they are estimated using analytical expressions provided by Eurocode [44] and simulated accordingly. The reinforcement is simulated as a bilinear hardening material, with a yield strength of 500 MPa and an ultimate strength of 550 MPa, consistent with the properties of B500 steel employed in the experiments. The assumed ultimate strain capacity of the applied reinforcement is 4.5%, in accordance with the provisions of Eurocode [44]. To capture the ductility and bond slip behavior of the reinforcement, the Rebar-Concrete interface elements are defined using

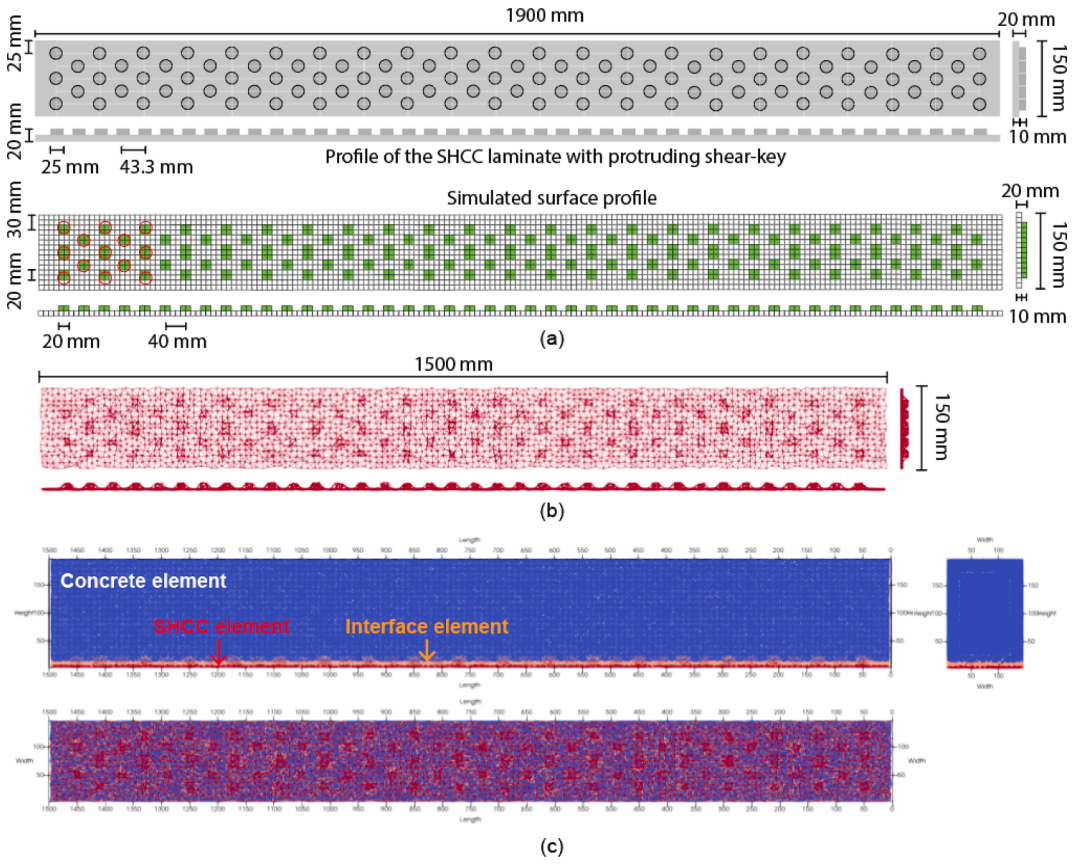

Fig. 15. (a) Comparison of the real profile and the simulated profile of the SHCC laminate with shear-key, (b) lattice model of a SHCC laminate with shear-key profile and (c) lattice model of the resulting hybrid beam with a profiled interface.

Table 4
Interface properties of performed six lattice simulations.

Simulation models	Property of interface elements as a fraction of concrete elements		
	Modulus E	Compressive strength f_c	Tensile strength f_t
R	–	–	–
S75	100%	100%	75%
P75	100%	100%	75%
P50	100%	100%	50%
P25	100%	100%	20%
P10	100%	100%	10%

15 segments, as outlined in Table 5. A similar elastoplastic definition for the Rebar-Concrete bond was utilized in a previous study [47].

The input properties of SHCC were determined from a simulated direct tension test on a 10 mm × 100 mm × 200 mm thin plate model (Fig. 16a), which has the same thickness as the SHCC layer in the hybrid beam model. SHCC is defined using 7 segments such that the modelled SHCC exhibits similar stress–strain response as obtained experimentally (Fig. 16b) with realistic multiple cracking behavior (Fig. 16b). The modelled SHCC also has good crack width control as shown by Fig. 16b, where the maximum crack width in SHCC at ultimate strain level is below 50 μm as commonly observed in experiments. However, the simulated SHCC has lower ductility (blue line) as compared to experiments (orange line), which might be because of the relatively large mesh size adopted in the study. As this study focuses more on analyzing the maximum crack width in SHCC rather than ductility, the modeling approach described earlier has been selected. However, it is worth noting that this approach may underestimate the ductility of the simulated hybrid beams.

In order to simplify the inputs for the SHCC/Concrete interface, the

Table 5
Material properties as inputs for lattice simulations.

Materials	Segment	Modulus E (GPa)	Tensile strength f_t (MPa)	Compressive strength f_c (MPa)
Concrete	–	32.00	4.0	70.0
SHCC	1	17.00	4.0	100.0
	2	10.00	3.5	0.1
	3	0.30	2.5	0.1
	4	0.20	2.5	0.1
	5	0.15	3.0	0.1
	6	0.12	4.0	0.1
	7	0.10	4.0	0.1
Reinforcement	1	200.00	500.0	500.0
	2	22.00	525.0	525.0
	3	12.00	550.0	550.0
Reinforcement/ Concrete Interface	1	47.00	6.0	6.0
	2	9.00	12.0	12.0
	3	4.44	17.0	17.0
	4	2.00	23.0	23.0
	5	1.00	29.0	29.0
	6	0.70	35.0	35.0
	7	0.50	40.0	40.0
	8	0.40	46.0	46.0
	9	0.30	52.0	52.0
	10	0.20	58.0	58.0
	11	0.10	58.0	58.0
	12	0.05	48.0	48.0
	13	0.03	39.0	39.0
	14	0.02	29.0	29.0
	15	0.01	20.0	20.0

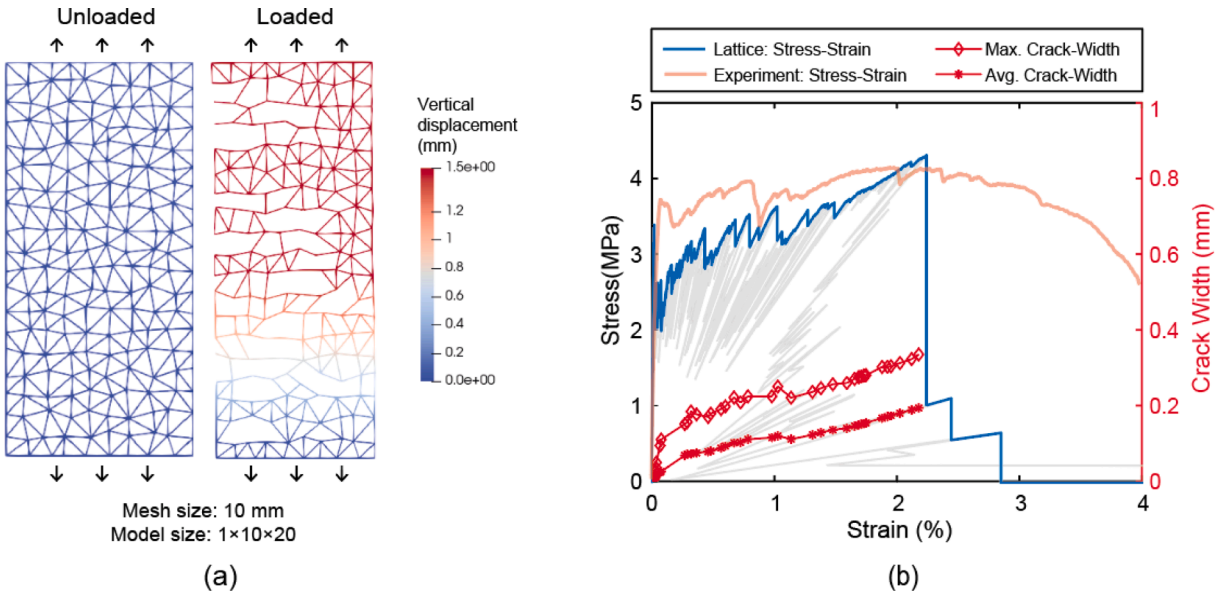

Fig. 16. (a) Lattice model of a uniaxial tensile test for the calibration of SHCC material properties and (b) comparison of simulated and tested stress–strain response.

strength values of the interface elements are expressed as a percentage of the strengths of concrete elements. The stiffness of the interface is kept the same as that of concrete. For simulation of the hybrid beams with smooth (S75) and untreated profiled interface (P75), the tensile strength of interface elements is assigned as 75% of the concrete properties. The remaining three hybrid beams have interface elements with decreasing tensile strength of 50% (P50), 25% (P25) and 10% (P10) of the tensile strength of concrete elements, while the compressive strength of interface elements in all simulated beams is assigned as 100% of the concrete properties. Assigning higher strength in compression is to simulate the condition of a physical contact, in which the interface is, in theory, able to transfer infinite load, as long as the materials on both sides do not fail.

4.3. Simulation results

The results of the simulation for reference reinforced concrete beam (R) are considered for verification of the model. The load–deflection-maximum crack width response of tested and simulated reinforced concrete beam is compared in Fig. 17a. It can be seen that the selected modeling choices are in general able to simulate the load deformation response, despite the fact that the model has slightly overestimated the stiffness of the beam after concrete cracking. Also, the simulated maximum crack widths are in good agreement as compared to experimental observations throughout the loading. Since crack width prediction and general insight into fracture behavior are the aims of this study, the described modeling approach was thus adopted. Because of the same reason, the simulations were only continued until the deflection reached 15 mm, as the max crack widths always exceed 0.3 mm at a deflection smaller than 15 mm. Fig. 17b shows the load-deformation results of all simulated beams. It can be seen that the influence of the SHCC layer and the interface properties can hardly be noticed, which is in agreement with the experimental observation as shown by Fig. 6a. Fig. 18 show the damage patterns from the lattice simulation for the reference beam R (Fig. 18a) and for the hybrid beam with the weakest profiled interface P10 (Fig. 18b). If these patterns are compared with the DIC results of Ref beam and Vaseline beam, it can be seen that the lattice simulations are able to develop similar crack pattern, with accurate crack spacing and crack number in the constant moment region. The debonding between the concrete and the SHCC in the Vaseline beam as observed by DIC is also well captured by the lattice simulation (Fig. 18b). Furthermore, the formation of multiple cracks in SHCC as observed from the bottom of the simulation is also consistent with the large number of cracks (Fig. 13a) as counted by DIC, which again proves the applicability of the current modeling approach.

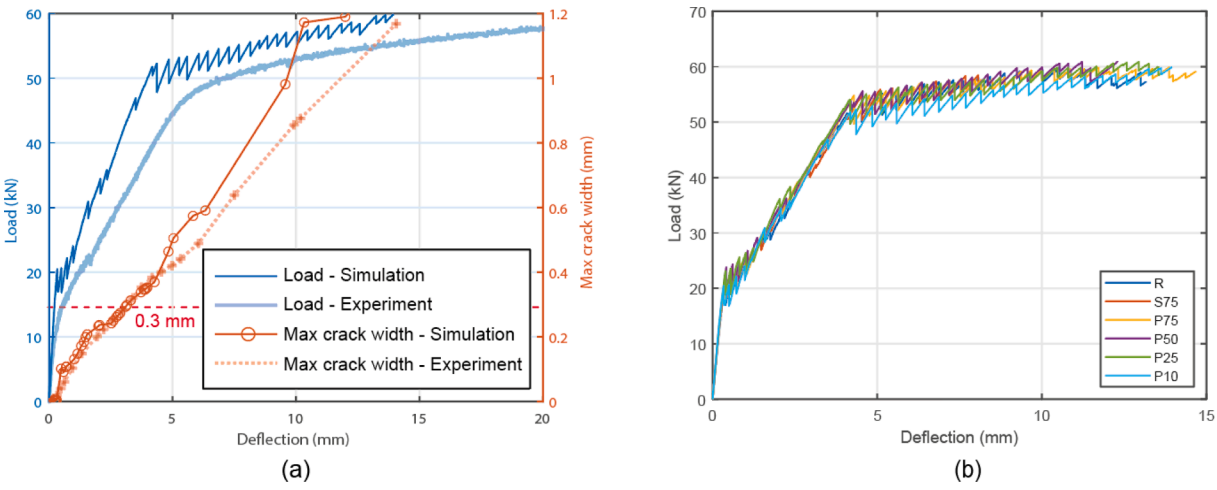

Fig. 17. (a) Comparison of simulation results and experimental results for the reference beam and (b) load deflection responses of all simulated beams.

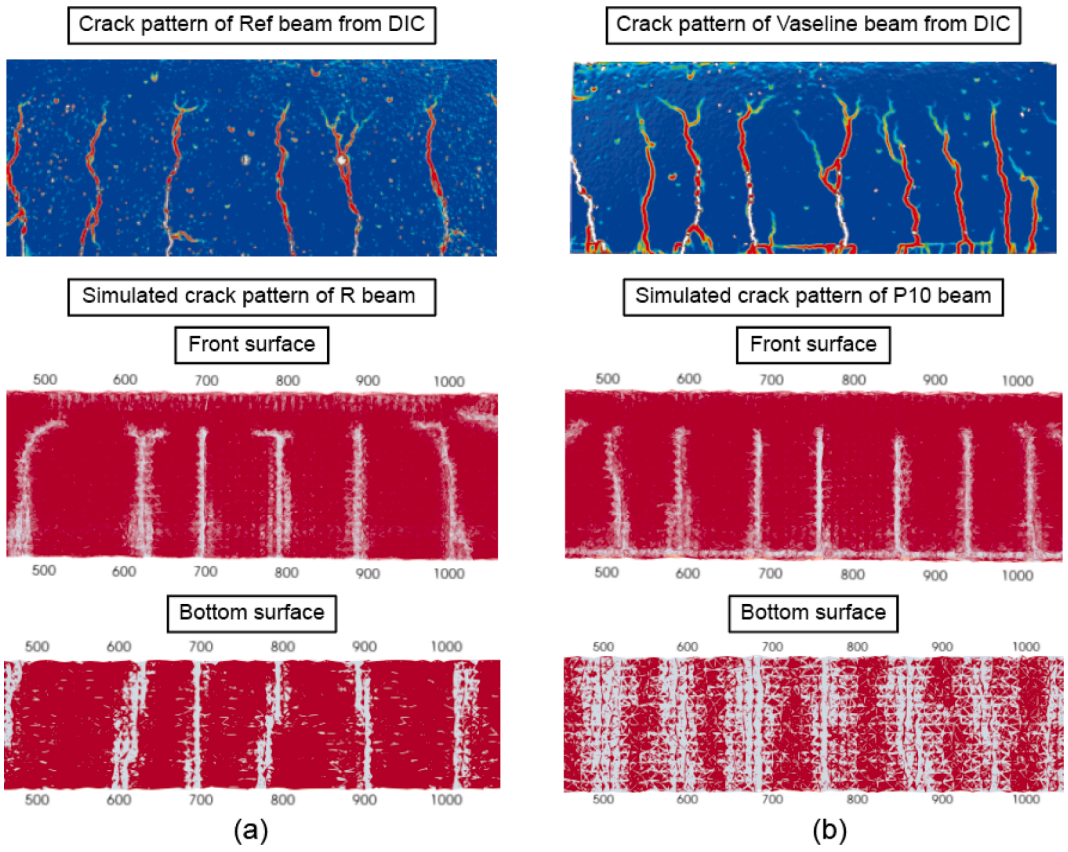

Fig. 18. Comparison of crack patterns from DIC and lattice model for (a) Ref beam and (b) Vaseline hybrid beam.

Fig. 19 shows the development of maximum crack width for all the simulations. The reference beam R has the largest crack width for all the deformations, followed by the hybrid beam with smooth interface. The simulation results of the profiled hybrid beams (P75-P10) demonstrate clearly that, by reducing the tensile strength of the interface elements, the development of the maximum crack width can be delayed. The profiled hybrid beam with the lowest tensile strength has the best crack width control performance among the six simulated beams. Fig. 20 shows the crack pattern of the simulated beam. A clear trend can be seen that, by gradually reducing the tensile strength of the interface elements, the degree of delamination increases, leading to the formation of more cracks in the SHCC. Fig. 21 shows the damage condition of only the interface elements and the SHCC elements. It can be found that a lower tensile strength results in the damage of more interface elements, and the number of cracks formed in SHCC increases with decreasing strength of the interface. To conclude, the simulation results demonstrate that, when the mechanical interlocking is provided, a weak interfacial bond between SHCC and concrete can indeed promote the activation of more SHCC and thus results in the formation of more cracks and a delayed development of maximum crack width.

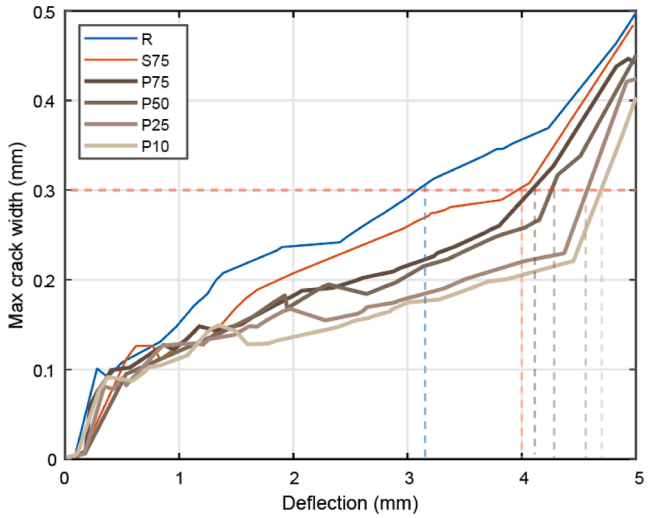

Fig. 19. Development of the maximum crack width for all the simulated beams.

5. Conclusion

A combined experimental and numerical study was performed aiming to investigate the cracking behavior of hybrid reinforced concrete beams enhanced with a very thin layer of SHCC in the cover zone, and also to verify the performance of a newly developed interface profile. Structural behavior, crack pattern and crack width development of the hybrid beams with different interface were tested and compared to the control reinforced concrete beams. The main findings of the current study are:

1. A 1-cm-thick SHCC layer can be very effective in controlling the crack width of a hybrid beam, as long as the interface is properly designed. As the volume ratio of SHCC used in the hybrid beams is only 6%, the current study demonstrates the feasibility of using minimum amount of SHCC in the critical region to efficiently enhance the performance of hybrid structures.
2. With a 1-cm-thick layer of SHCC, the maximum crack width of the best performing hybrid beam exceeded 0.3 mm at 53.3 kN load, whereas in the control beam the largest crack exceeded 0.3 mm at only 32.5 kN load. This 64% increase in load at the critical crack width means that the amount of reinforcement can be largely

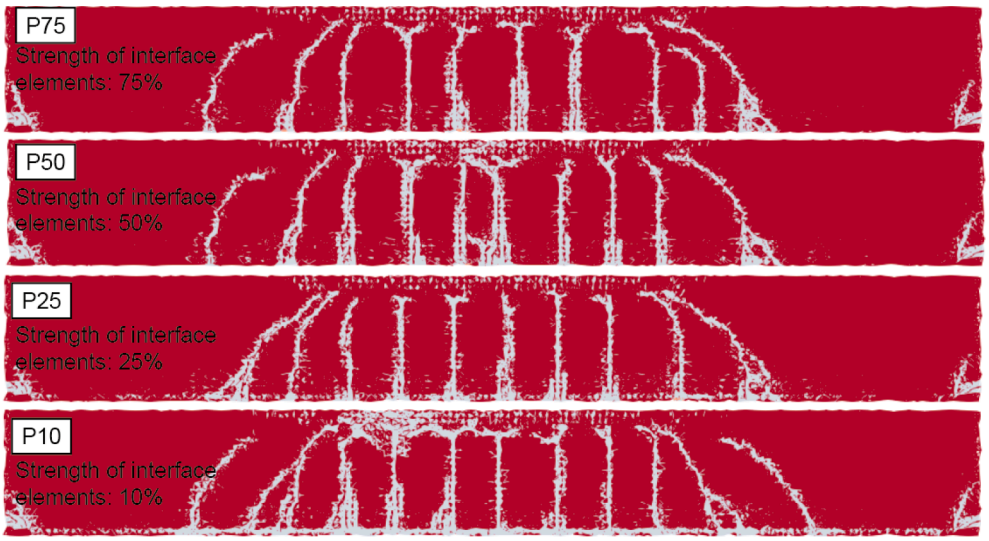

Fig. 20. Simulated crack pattern of hybrid beams with interface element having different tensile strength (front view).

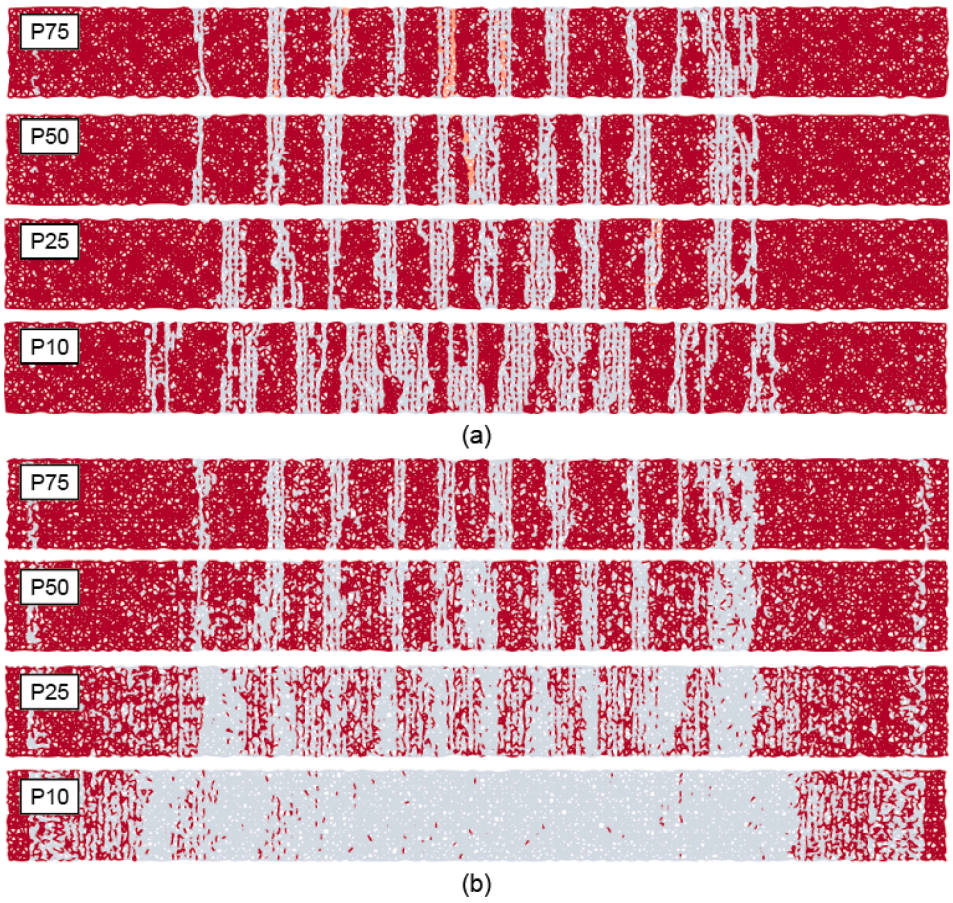

Fig. 21. Simulated damage condition of (a) SHCC elements and (b) interface elements of hybrid beams with interface element having different tensile strength (bottom view).

reduced, if the excess reinforcement is not necessary for structural capacity.

3. A smooth interface is not desirable as it can only marginally delay the crack width development. The hybrid beams with a profiled interface have much improved crack width control ability. The proposed new SHCC/concrete interface that features a weakened chemical adhesion but an enhanced mechanical bonding can successfully lead to a controlled extent of partial delamination between the two layers, which promotes the activation of SHCC. The hybrid beam with the proposed new interface formed 10 times more cracks in SHCC than a hybrid beam with a simple smooth interface and had an average crack width less than 0.1 mm for all deflection levels.
4. The lattice model has demonstrated its capability to predict and provide insight into the fracture behavior of hybrid systems. It can

accurately simulate both the crack development and the load–deflection response. The simulation results suggest that, when the mechanical interlocking is provided, a weak interface bond can indeed promote the activation of more SHCC and thus results in the formation of more cracks as well as a delayed development of maximum crack width.

5. The hybrid beams developed in the current study possess an improved crack control ability at the expense of minimal additional cost. The reduced crack width is expected to increase the durability and the self-healing potential of the structural elements, which may eventually lead to an extended service life of the whole structure.

CRediT authorship contribution statement

Shan He: Conceptualization, Methodology, Data curation, Formal analysis, Investigation, Writing – original draft, Visualization. **Shozab Mustafa:** Investigation, Software, Validation, Writing – review & editing. **Ze Chang:** Investigation, Software, Writing – review & editing. **Minfei Liang:** Investigation, Data curation, Writing – review & editing. **Erik Schlangen:** Conceptualization, Project administration, Funding acquisition, Supervision, Writing – review & editing. **Mladena Luković:** Conceptualization, Project administration, Resources, Supervision, Writing – review & editing.

Declaration of Competing Interest

The authors declare that they have no known competing financial interests or personal relationships that could have appeared to influence the work reported in this paper.

Data availability

Data will be made available on request.

Acknowledgement

Shan He acknowledges the financial support from the MSCA-ITN project SMARTINCS. This project has received funding from the European Union's Horizon 2020 research and innovation programme under the Marie Skłodowska-Curie grant agreement No 860006. Ze Chang and Minfei Liang would like to acknowledge the funding supported by China Scholarship Council under grant number 201806060129 and 202007000027. Mladena Luković would also like to acknowledge the Dutch Organization for Scientific Research (NWO) for the grant "Optimization of interface behavior for innovative hybrid concrete structures" (project number 16814).

References

[1] Tiberti G, Minelli F, Plizzari G. Cracking behavior in reinforced concrete members with steel fibers: A comprehensive experimental study. Cem Concr Res 2015;68:24–34. https://doi.org/10.1016/J.CEMCONRES.2014.10.011.
[2] Rokugo Tetsushi Kanda AE Hiroshi Yokota AE Noboru Sakata KA. Applications and recommendations of high performance fiber reinforced cement composites with multiple fine cracking (HPFRCC) in Japan n.d. https://doi.org/10.1617/s11527-009-9541-8.
[3] He S, Yang EH. Non-normal distribution of residual flexural strengths of steel fiber reinforced concretes and its impacts on design and conformity assessment. Cem Concr Compos 2021;123:104207. https://doi.org/10.1016/J.CEMCONCOMP.2021.104207.
[4] di Prisco M, Plizzari G, Vandewalle L. Fibre reinforced concrete: New design perspectives. Materials and Structures/Materiaux et Constructions 2009;42:1261–81. https://doi.org/10.1617/S11527-009-9529-4/FIGURES/15.
[5] Li VC. On Engineered Cementitious Composites (ECC) a review of the material and its applications. J Adv Concr Technol 2003;1:215–30. https://doi.org/10.3151/JACT.1.215.
[6] Li VC. Engineered Cementitious Composites (ECC). Engineered Cementitious Composites (ECC) 2019. https://doi.org/10.1007/978-3-662-58438-5.
[7] Li VC. Tailoring ECC for Special Attributes: A Review. Int J Concr Struct Mater 2012;6:135–44. https://doi.org/10.1007/S40069-012-0018-8.
[8] Zhang Y, Bai S, Zhang Q, Xie H, Zhang X. Failure behavior of strain hardening cementitious composites for shear strengthening RC member. Constr Build Mater 2015;78:470–3. https://doi.org/10.1016/J.CONBUILDMAT.2015.01.037.
[9] Khalil AEH, Etman E, Atta A, Essam M. Behavior of RC beams strengthened with strain hardening cementitious composites (SHCC) subjected to monotonic and repeated loads. Eng Struct 2017;140:151–63. https://doi.org/10.1016/J.ENGSTRUCT.2017.02.049.
[10] Luković M, Hordijk DA, Huang Z, Schlangen E. Strain hardening cementitious composite (SHCC) for crack width control in reinforced concrete beams. Heron 2019;64:189–206.
[11] Khan MI, Sial SU, Fares G, ElGawady M, Mourad S, Alharbi Y. Flexural performance of beams strengthened with a strain-hardening cementitious composite overlay. Case Studies. Constr Mater 2022:17. https://doi.org/10.1016/J.CSCM.2022.E01645.
[12] Leung CKY, Cao Q. Development of Pseudo-ductile permanent formwork for durable concrete structures. Materials and Structures/Materiaux et Constructions 2010;43:993–1007. https://doi.org/10.1617/S11527-009-9561-4/FIGURES/17.
[13] Ge W-J, Ashour AF, Yu J, Gao P, Cao D-F, Cai C, et al. Flexural behavior of ECC–concrete hybrid composite beams reinforced with FRP and steel bars. J Compos Constr 2019;23:04018069.
[14] Ge W, Ashour AF, Cao D, Lu W, Gao P, Yu J, et al. Experimental study on flexural behavior of ECC-concrete composite beams reinforced with FRP bars. Compos Struct 2019;208:454–65. https://doi.org/10.1016/j.compstruct.2018.10.026.
[15] Ge W, Song W, Ashour AF, Lu W, Cao D. Flexural performance of FRP/steel hybrid reinforced engineered cementitious composite beams. Journal of Building Engineering 2020;31:101329. https://doi.org/10.1016/j.jobe.2020.101329.
[16] Sheta A, Ma X, Zhuge Y, ElGawady M, Mills J, Abd-Elaal E. Flexural strength of innovative thin-walled composite cold-formed steel/PE-ECC beams. Eng Struct 2022;267:114675. https://doi.org/10.1016/j.engstruct.2022.114675.
[17] Sheta A, Ma X, Zhuge Y, ElGawady MA, Mills JE, Singh A, et al. Structural performance of novel thin-walled composite cold-formed steel/PE-ECC beams. Thin-Walled Struct 2021;162:107586. https://doi.org/10.1016/j.tws.2021.107586.
[18] Sheta A, Ma X, Zhuge Y, ElGawady M, Mills JE, Abd-Elaal E. Axial compressive behaviour of thin-walled composite columns comprise high-strength cold-formed steel and PE-ECC. Thin-Walled Struct 2023;184:110471. https://doi.org/10.1016/j.tws.2022.110471.
[19] Deng BY, Tan D, Li LZ, Zhang Z, Cai ZW, Yu KQ. Flexural behavior of precast ultra-lightweight ECC-concrete composite slab with lattice girders. Eng Struct 2023;279:115553. https://doi.org/10.1016/J.ENGSTRUCT.2022.115553.
[20] Mustafa S, Singh S, Hordijk D, Schlangen E, Luković M. Experimental and numerical investigation on the role of interface for crack-width control of hybrid SHCC concrete beams. Eng Struct 2022:251. https://doi.org/10.1016/j.engstruct.2021.113378.
[21] Qian SZ, Li VC, Zhang H, Keoleian GA. Life cycle analysis of pavement overlays made with Engineered Cementitious Composites. Cem Concr Compos 2013;35:78–88. https://doi.org/10.1016/J.CEMCONCOMP.2012.08.012.
[22] Baloch WL, Siad H, Lachemi M, Sahmaran M. A review on the durability of concrete-to-concrete bond in recent rehabilitated structures. Journal of Building Engineering 2021;44:103315. https://doi.org/10.1016/j.jobe.2021.103315.
[23] Apostolinas VG, Galopoulou KS, Kouris LAS, Anastasiou EK, Konstantinidis AA. Experimental investigation and analytical modelling of the roughness and bonding agent influence on the old-to-repair concrete interfacial bonding strength. Mater Struct 2022;55:148. https://doi.org/10.1617/s11527-022-01984-y.
[24] Sadowski Ł. Adhesion in Layered Cement Composites. Springer; 2019.
[25] Mladena L. Influence of interface and strain hardening cementitious composite (SHCC) properties on the performance of concrete repairs. Delft University of Technology; 2016.
[26] Xiong G, Luo B, Wu X, Li G, Chen L. Influence of silane coupling agent on quality of interfacial transition zone between concrete substrate and repair materials. Cem Concr Compos 2006;28:97–101. https://doi.org/10.1016/j.cemconcomp.2005.09.004.
[27] Zhang R, Hu P, Zheng X, Cai L, Guo R, Wei D. Shear behavior of RC slender beams without stirrups by using precast U-shaped ECC permanent formwork. Constr Build Mater 2020;260:120430. https://doi.org/10.1016/J.CONBUILDMAT.2020.120430.
[28] Kunieda M, Kamada T, Rokugo K. Localized fracture of repair material in patch repair systems. Proceedings of FRAMCOS-5, Vail, Colorado, USA: 2004.
[29] Suryanto B, Nagai K, Maekawa K. Modeling and analysis of shear-critical ECC members with anisotropic stress and strain fields. J Adv Concr Technol 2010;8:239–58.
[30] Han T-S, Feenstra PH, Billington SL. Simulation of highly ductile fiber-reinforced cement-based composite components under cyclic loading. Structural Journal 2003;100:749–57.

[31] Kabele P. Multiscale framework for modeling of fracture in high performance fiber reinforced cementitious composites. Eng Fract Mech 2007;74:194–209. https://doi.org/10.1016/j.engfracmech.2006.01.020.
[32] Baloch H, Grünewald S, Matthys S. Different Approaches for FEM Modelling of Strain-Hardening Cementitious Composites. In: Serna P, Llano-Torre A, Martí-Vargas JR, Navarro-Gregori J, editors. Fibre Reinforced Concrete: Improvements and Innovations II. Cham: Springer International Publishing; 2022. p. 389–99.
[33] Shehni A. Modeling of Strain-Hardening Cement-based Composites (SHCC) 2020.
[34] Schlangen E, van Mier JGM. Simple lattice model for numerical simulation of fracture of concrete materials and structures. Mater Struct 1992;25:534–42. https://doi.org/10.1007/BF02472449/METRICS.
[35] Schlangen E. M&S highlight: Schlangen and van Mier (1992), Simple lattice model for numerical simulation of fracture of concrete materials and structures. Materials and Structures/Materiaux et Constructions 2022;55. https://doi.org/10.1617/S11527-022-01932-W.
[36] Chang Z, Zhang H, Schlangen E, Šavija B. Lattice Fracture Model for Concrete Fracture Revisited: Calibration and Validation. Applied Sciences. 2020;10:4822. https://doi.org/10.3390/APP10144822.
[37] Šavija B, Pacheco J, Schlangen E. Lattice modeling of chloride diffusion in sound and cracked concrete. Cem Concr Compos 2013;42:30–40. https://doi.org/10.1016/J.CEMCONCOMP.2013.05.003.
[38] The MSCA-ITN project SMARTINCS. Homepage available at www.smartincs.eu from 2020.
[39] He S, Zhang S, Luković M, Schlangen E. Effects of bacteria-embedded polylactic acid (PLA) capsules on fracture properties of strain hardening cementitious composite (SHCC). Eng Fract Mech 2022;268:108480. https://doi.org/10.1016/J.ENGFRACMECH.2022.108480.
[40] Zhou J, Qian S, Beltran MGS, Ye G, van Breugel K, Li VC. Development of engineered cementitious composites with limestone powder and blast furnace slag. Materials and Structures/Materiaux et Constructions 2010;43:803–14. https://doi.org/10.1617/s11527-009-9549-0.
[41] Testing of hardened concrete - Part 3: Compressive strength of test pieces. NEN-EN 12930-3. Testing of hardened concrete - Part 3: Compressive strength of test pieces. 2019.
[42] European committee for standardization. NEN-EN 196-1. Methods of testing cement - Part 1: Determination of strength. 2016.
[43] Japan Society of Civil Engineers. Recommendations for Design and Construction of High Performance Fiber Reinforced Cement Composites with Multiple Fine Cracks (HPFRCC). 2008.
[44] European Committee for Standardization. EN 1992-1-1 Eurocode 2: Design of Concrete Structures - Part I: General Rules and Rules for Buildings. 2011.
[45] Šavija B, Luković M, Schlangen E. Influence of Cracking on Moisture Uptake in Strain-Hardening Cementitious Composites. J Nanomech Micromech 2017:7. https://doi.org/10.1061/(ASCE)NM.2153-5477.0000114.
[46] Chang Z, Xu Y, Chen Y, Gan Y, Schlangen E, Šavija B. A discrete lattice model for assessment of buildability performance of 3D-printed concrete. Comput Aided Civ Inf Eng 2021;36:638–55. https://doi.org/10.1111/MICE.12700.
[47] Gu D, Mustafa S, Pan J, Luković M. Reinforcement-concrete bond in discrete modeling of structural concrete. Comput Aided Civ Inf Eng 2022. https://doi.org/10.1111/mice.12937.